IOPscience iopscience.iop.org

Home Search Collections Journals About Contact us My IOPscience

Size effects on the thermal conductivity of polycrystalline platinum nanofilms

This article has been downloaded from IOPscience. Please scroll down to see the full text article.

2006 J. Phys.: Condens. Matter 18 7937

(http://iopscience.iop.org/0953-8984/18/34/007)

View the table of contents for this issue, or go to the journal homepage for more

Download details:
IP Address: 129.252.86.83
The article was downloaded on 29/05/2010 at 08:03

Please note that terms and conditions apply.

INSTITUTE OF PHYSICS PUBLISHING JOURNAL OF PHYSICS: CONDENSED MATTER

J. Phys.: Condens. Matter **18** (2006) 7937–7950 doi:10.1088/0953-8984/18/34/007

Size effects on the thermal conductivity of polycrystalline platinum nanofilms

Q G Zhang[1], B Y Cao[1], X Zhang[1,4], M Fujii[2] and K Takahashi[3]

[1] Key Laboratory for Thermal Science and Power Engineering of Ministry of Education, Department of Engineering Mechanics, Tsinghua University, Beijing 100084, People's Republic of China
[2] Institute for Materials Chemistry and Engineering, Kyushu University, Kasuga 816-8580, Japan
[3] Graduate School of Engineering, Kyushu University, Fukuoka 812-8581, Japan

E-mail: x-zhang@tsinghua.edu.cn

Received 22 April 2006, in final form 1 July 2006
Published 7 August 2006
Online at stacks.iop.org/JPhysCM/18/7937

Abstract

The surface and grain-boundary effects on the in-plane thermal conductivity of polycrystalline platinum nanofilms have been investigated. The thicknesses of the nanofilms range from 15.0 to 63.0 nm and the mean grain sizes measured by x-ray diffraction vary from 9.5 to 26.4 nm. The thermal conductivities of the nanofilms measured by a direct electrical heating method are greatly reduced from the bulk values. The measured results are compared with the values predicted by the Qiu and Tien model and the Kumar and Vradis theory. It is found that the reduction in the thermal conductivity is mainly caused by grain-boundary scattering and the reflection coefficient of electrons striking the grain boundaries is around 0.35. The relaxation time model is also applied to study the size effects to check whether the Matthiessen rule is still valid in predicting the in-plane thermal conductivity of polycrystalline metallic nanofilms. The results indicate that by considering only grain-boundary scattering and background scattering the Matthiessen rule is still valid. If surface scattering, however, is included, deviations of the Matthiessen rule from other theories mentioned above have been found.

1. Introduction

Studies on the thermal conductivity of metallic thin films have attracted tremendous interest over past decades due to their wide applications as interconnects in modern ultra-large-scale integrated (ULSI) circuits. As the dimension of the metallic interconnects is decreased comparable to the electron mean free path, size effects on the thermal transport process will

[4] Author to whom any correspondence should be addressed.

 © 2006 IOP Publishing Ltd Printed in the UK

become important, which usually leads to a reduction of the thermal conductivity of the metallic thin films. Such a reduction will then worsen the heat transfer in the ULSI circuits, and even lead to the burnout of the chips.

Difficulties in directly measuring the thermal conductivity of the metallic thin films according to the Fourier law exist, since the imposed heat flux is generally very small and the temperature distribution is considerably difficult to detect. A few indirect methods have been put forward, such as the steady state method [1–4], the pulse method [5], the picosecond thermoreflectance method [6], the photoacoustic method [7] and the ac calorimetric method [8] to measure the in-/out-of-plane thermal conductivity or thermal diffusivity of metallic thin films. The existing experimental results show that the thermal conductivity is much reduced from the corresponding bulk values, even down to one order of magnitude. Such a reduction is mainly attributed to the size effects on the scattering processes of conduction electrons in metallic systems, due to the surface [1–8] and the grain boundary [8].

Theoretical studies on the surface and grain-boundary effects have also been carried out in the past several decades. By applying the electrical–thermal analogy introduced by the Wiedemann–Franz law, Tien *et al* [9] and Qiu *et al* [10] firstly studied the surface and grain-boundary effects on the thermal conductivity of metallic thin films. Their work is mainly based on the Fuchs–Sondheimer (FS) [11, 12] theory to study the surface effect and the Mayadas–Shatzkes (MS) [13, 14] theory to study the grain-boundary effect. If the ratio between the thickness and the mean grain size is taken to be 5.0 and the reflection coefficient of electrons striking the grain boundaries is taken to be 0.23, the predictions made by the Qiu and Tien model agree well with the experimental results in [3]. Since the Wiedemann–Franz law for bulk metals has not been proved for metallic thin films, Kumar and Vradis [15] directly studied the surface effect on the thermal conductivity of single-crystal metallic films. The results show that the leading order behaviour of the ratios of film thermal and electrical conductivities to their corresponding bulk values is identical. With a relaxation time model, Kumar and Vradis also considered the grain-boundary effect on the thermal conductivity of polycrystalline metallic thin films. If the mean grain size is taken to be equal to the corresponding thickness, the calculated results also coincide with the experimental results in [3]. Therefore, the discrepancy is found that different relationships between the mean grain size and the film thickness have been obtained, when the Kumar and Vradis (KV) theory and the Qiu and Tien model are compared with the same experiment in [3]. In the previous work, to our knowledge, the relative magnitudes of the surface and grain-boundary effects on the thermal conductivity of metallic thin films have not yet been discussed.

The Matthiessen rule [16] can be readily applied to estimate the relative magnitude of different scattering mechanisms. It has been widely used to predict the phonon thermal conductivity of dielectric solids [17] and the electrical conductivity or electronic thermal conductivity of metallic materials [16]. However, the work of Mayadas and Shatzkes shows that the total in-plane electrical resistivity of the polycrystalline metallic thin films exhibits a deviation from the Matthiessen rule, and the electrical resistivity of the polycrystalline metals cannot be expressed as the sum of a resistivity due solely to grain boundaries and the background resistivity [14]. Durkan also pointed out that in the presence of background and surface/grain-boundary scattering, the Matthiessen rule is not satisfied in evaluating the electrical resistivity of polycrystalline nanowires [18]. It is still an open question, however, whether the Matthiessen rule is still valid in predicting the thermal conductivity of metallic thin films.

The in-plane thermal conductivity of polycrystalline metallic nanofilms is investigated experimentally and theoretically in this paper to illustrate the relative importance of the surface and grain-boundary effects on the reduction of the thermal conductivity, and to examine

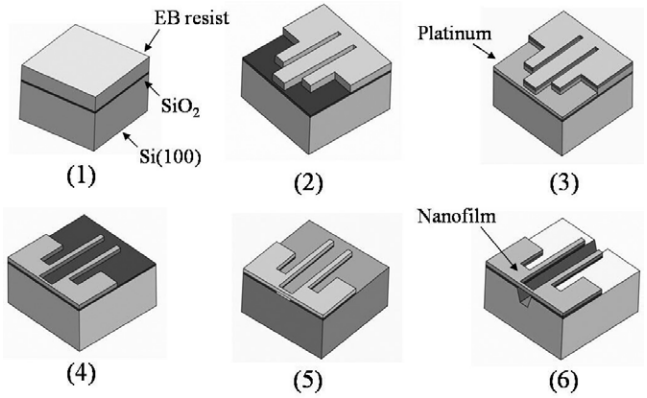

Figure 1. Schematic fabrication processes of the platinum nanofilms.

the applicability of the Matthiessen rule in predicting the in-plane thermal conductivity of polycrystalline metallic thin films.

2. Experiment

2.1. Preparation of the platinum nanofilms

In order to measure the thermal conductivities of the platinum nanofilms with a direct electrical heating method [19, 20], the nanofilms need to be connected with four leads and to be suspended from their substrate. The nanofilms are fabricated by electron beam (EB) lithography, electron beam–physical vapour deposition (EB-PVD) and isotropic/anisotropic etching techniques. The fabrication processes, as shown in figure 1, are listed as follows. (1) The Si(100) substrate with a SiO_2 layer of 180 nm thickness is used as the starting material. An EB resist is spin-coated to be 320 nm in thickness. (2) By using the EB lithography system, patterns of the nanofilm and leads are directly drawn on the EB resist. (3) Titanium and platinum films are deposited sequentially by the EB-PVD method. The thickness of the titanium film, which is used only for adhesion, is usually taken to be 5.0 nm, while the thickness of the platinum film ranges from 15.0 to 63.0 nm. When the thickness is larger than 40.0 nm, the deposition rate has been increased from 0.08 to 0.10–0.11 nm s^{-1}. (4) The lift-off technique is applied, where the chip is immersed in the liquid resist-remover to leave only Pt/Ti pattern on the SiO_2 layer. (5) The isotropic etching using the buffered hydrofluoric acid is applied to remove the SiO_2 layer around the nanofilm. Titanium is also etched away in this process. (6) Si is anisotropically etched using KOH solution in order to detach the nanofilm from the substrate, and the gap between the nanofilm and the substrate is about 6 μm. The size parameters of the fabricated nanofilms are listed as in table 1. Previous studies indicate that the thermal conductivity of the nanofilms is independent of the width [20], and can then be characterized only by the nanofilm thickness.

2.2. Principle of the measurement

Figure 2 shows the physical model of the direct electrical heating method. In this method, the metallic nanofilm serves both as heater and resistance thermometer, which is different from the well known 3ω method [21, 22] in principle. The metallic thin film in the 3ω method is just used

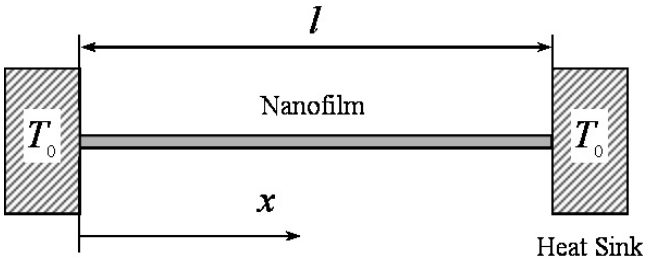

Figure 2. Physical model of the direct electrical heating method.

Table 1. The size parameters of the fabricated platinum nanofilms.

Nanofilm sample	(1)	(2)	(3)	(4)	(5)	(6)	(7)	(8)	(9)
Thickness δ (nm)	15.0	22.0	24.0	27.5	27.8	40.0	62.0	62.0	63.0
Width w (nm)	495.8	479.6	491.1	260.0	479.6	362.0	1383.4	1228.0	696.8
Length l (μm)	8.92	5.56	5.83	5.30	5.56	5.67	9.21	8.87	6.23
Grain size d (nm)	9.5	11.4	11.6	19.2	18.8	26.4	16.3	14.8	17.6

as heater and temperature sensor and the out-of-plane thermal conductivity of the underlying dielectric films is measured, while in the present method the in-plane thermal conductivity of the metallic nanofilm itself is the objective to be studied.

Initially, the nanofilm and the heat sinks (i.e. the leads) are maintained in thermal equilibrium at a set temperature of T_0. As a direct current flows through the nanofilm, the generated joule heat will lead to a temperature rise of the nanofilm. In consideration of the great difference in the heat capacity of the nanofilm and that of the heat sinks, the temperature distribution along the nanofilm will reach a steady state within several microseconds after heating. Since all the measurements are carried out at a high vacuum level of $\sim 3 \times 10^{-6}$ Torr and at the set temperatures ranging from 80 to 300 K, the residual gas heat conduction and thermal radiation loss can be ignored. Therefore, the heat transfer through the nanofilm can be simplified into one-dimensional steady-state heat conduction. The heat sinks are always maintained with a constant temperature T_0 during the measurement. The temperature distribution along the nanofilm can then be obtained, which is expressed by

$$T(x) = T_0 + \frac{IV}{2w\delta\lambda_f}x - \frac{IV}{2lw\delta\lambda_f}x^2, \tag{1}$$

where x is the distance from the left lead, I and V are the current and voltage applied on the nanofilm respectively, l is the length, w is the width, δ is the thickness, and λ_f is the required thermal conductivity of the nanofilms. As the heating power IV is only several microwatts, the maximum temperature rise does not exceed 10 K. The average temperature increase of the nanofilm ΔT_L can be deduced from equation (1) as

$$\Delta T_L = \frac{IV}{\lambda_f}\frac{l}{12w\delta}. \tag{2}$$

Such a temperature rise will lead to an increase in the resistance of the nanofilm R_f through

$$R_f = R_0 + \beta R_0 \Delta T_L, \tag{3}$$

where R_0 is the resistance at the set temperature T_0, and β is the temperature coefficient of resistance (TCR) at T_0. By combining equations (2) and (3), we can obtain the relationship

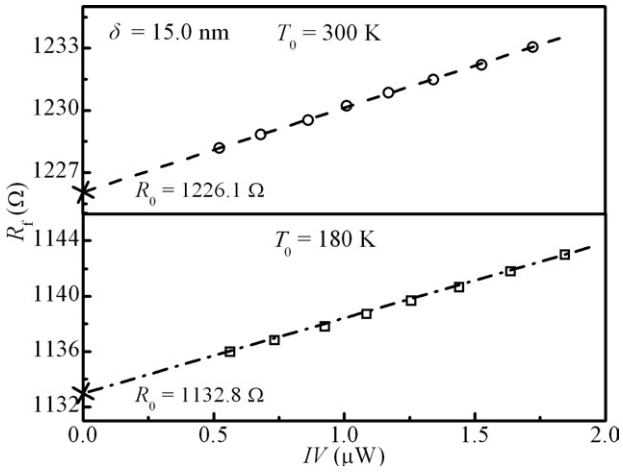

Figure 3. The variations of the nanofilm resistance along the heating power at the set temperature (a) 300 K and (b) 180 K. The thickness of the nanofilm is 15.0 nm.

between the increased resistance R_f and the heating power IV as

$$R_f = R_0 + \frac{\beta R_0}{\lambda_f} \frac{l}{12w\delta} IV. \tag{4}$$

Since the increased resistance can be calculated directly through the voltage divided by the current, i.e. $R_f = V/I$, the above relationship can also be achieved from the experimental data. Figure 3 shows the variation of measured resistance along the heating power at the set temperature 300 and 180 K, respectively, for the 15.0 nm thick nanofilm. By extrapolating the heating power to be zero, the resistance R_0 at the set temperature T_0 can be readily obtained. Also we can obtain the slope of the resistance varying with the heating power, which is denoted as a for simplicity. By comparing with equation (4), we find that $a = (\beta R_0 l)/(12\lambda_f w\delta)$. Two unknown parameters in the slope are the TCR and the thermal conductivity of the nanofilm. The TCR can be calculated from calibration by

$$\beta = \frac{R_0 - R_r}{R_r (T_0 - T_r)}, \tag{5}$$

where R_r is the reference resistance of the nanofilm at the reference temperature T_r, which is usually taken to be 293.2 K. Figure 4 shows the variations of the resistance corresponding to zero power along the set temperature for the 15.0 and 62.0 nm thick nanofilms, respectively, from which the TCR at different set temperatures can be readily obtained. The thermal conductivity is then calculated through

$$\lambda_f = \frac{\beta R_0}{a} \frac{l}{12w\delta}. \tag{6}$$

It is found from figure 3 that the resistance and the heating power are in a good linear relationship, the same as the theoretical analysis predicts as shown in equation (4). The accordance between the experimental results and the theoretical analysis has provided one proof to verify the present method.

We can find from equation (6) that the uncertainty of measuring the thermal conductivity comes from the measurement of the current, the voltage, and the dimension of the nanofilm. The current and the voltage are measured by two high accuracy digital multimeters (Keitheley 2002, 8.5 digits), and the relative uncertainty is not more than 16 ppm. The width and length

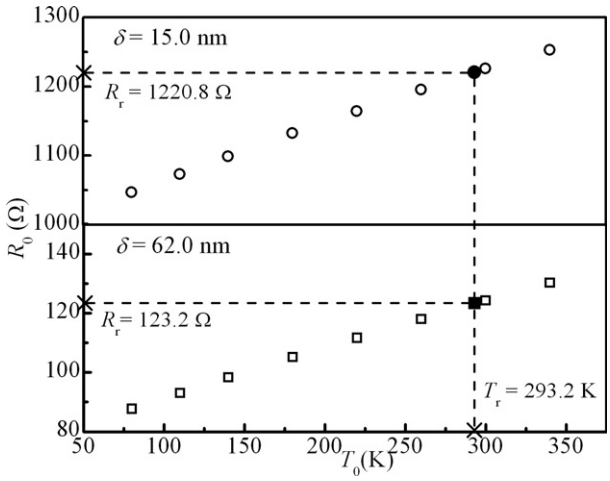

Figure 4. The variation of the nanofilm resistance corresponding to zero power along the set temperature. The thicknesses of the nanofilms are (a) 15.0 nm and (b) 62.0 nm.

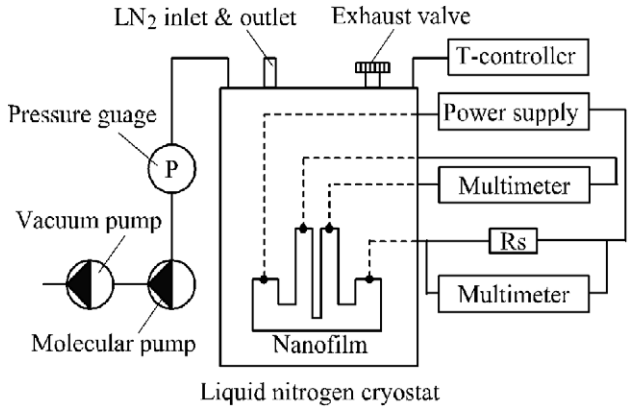

Figure 5. Schematic diagram of the experimental apparatus and measurement circuit.

of the nanofilm are measured with a scanning electron microscope (SEM). The thickness is measured with a calibrated quartz crystal thin-film thickness monitor (CRTM-7000 with the resolution of 0.01 nm) and an atomic force microscope (AFM). The total error caused by the dimension measurements is estimated to be less than ±3%. The total error is estimated to be within ±5%.

2.3. Experiment equipments

The schematic diagrams of the experimental apparatus and the measuring circuit are shown in figure 5. In all the measurements, the silicon chip with the suspended metallic nanofilm is mounted on the sample holder of a liquid nitrogen cryostat (Oxford Instruments, Optistat DN-V). The sample chamber is continuously evacuated by a vacuum pump and a molecular pump, and the temperature of the sample holder can be continuously controlled from 77 to 500 K. The measurement system consists of the nanofilm sample, two high accuracy digital multimeters

(Keithley 2002, 8.5 digits), a standard resistance (Yokogawa 2792) and a high accuracy power supply (Advantest R6243).

3. Theory

3.1. Surface effect

As the thickness of metallic thin films is comparable to or less than the electron mean free path (MFP), which is about 23 nm for platinum at 300 K, the effect of electron scatterings on the surface becomes evident. By solving the Boltzmann transport equation with surface scattering being a boundary condition, Fuchs and Sondheimer [11, 12] have studied the surface effect on the electrical conductivity of single-crystal metallic thin films. With the electrical–thermal transport analogy introduced by the Wiedemann–Franz law, Tien *et al* [9] obtained the ratio of film to bulk thermal conductivity as

$$\frac{\lambda_f}{\lambda_b} = 1 - \frac{3(1-p)}{2k}\int_1^\infty \left(\frac{1}{t^3} - \frac{1}{t^5}\right)\frac{1-\exp(-kt)}{1-p\exp(-kt)}\,dt, \tag{7}$$

where λ_f and λ_b are the film and bulk thermal conductivities respectively, p is the specularly reflected coefficient of electrons at the surface, and k is the ratio between the film thickness δ and the electron MFP of the bulk material l_b.

Kumar and Vradis [15] directly studied the surface effect on the in-plane thermal conductivity of single-crystal metallic thin films by solving the Boltzmann transport equation with a temperature gradient imposed along the film. The approximate expression for the ratio of film to bulk thermal conductivity can be written as

$$\frac{\lambda_f}{\lambda_b} = 1 - (1-p)^2\sum_{n=1}^{\infty} np^{n-1}\left[1 - \frac{3}{4}nk\,(1 - c - \ln(nk) + nk/2)\right], \qquad k \leqslant 1, \tag{8a}$$

$$\frac{\lambda_f}{\lambda_b} = 1 - \frac{3}{8}(1-p)\frac{1}{k}, \qquad k > 1, \tag{8b}$$

where $c = 0.577$ is Euler's constant used in the expansion of the exponential integral function.

By considering the background and surface scattering λ simultaneously, the effective relaxation time τ_f of single-crystal metallic thin films can be obtained from the Matthiessen rule as

$$\frac{1}{\tau_f} = \frac{1}{\tau_b} + \frac{1}{\tau_s}, \tag{9}$$

where $\tau_f = l_f/v_F$, $\tau_b = l_b/v_F$, $\tau_s = \delta/v_F$, τ_b is the relaxation time of the single-crystal bulk metals, τ_s is the relaxation time caused by surface scattering, l_f is the effective MFP of the films, l_b is the MFP of the single-crystal bulk metals, and v_F is the Fermi velocity. The expression for the ratio of film to bulk thermal conductivity can then be obtained as

$$\frac{\lambda_f}{\lambda_b} = \frac{l_f}{l_b} = \frac{1}{1 + l_b/\delta}. \tag{10}$$

The MFP of the bulk metals l_b can be related to the thermal conductivity λ_b by the formula [17]

$$\lambda_b = \frac{\pi^2 n k_B^2}{3mv_F} T l_b, \tag{11}$$

where m is the electron mass, n is the electron density, and k_B is the Boltzmann constant. With this formula, the variations of the thermal conductivity of metallic thin films with the thickness and with the temperature can be readily obtained from equations (7), (8) and (10).

3.2. Grain-boundary effect

As the metallic thin films are polycrystalline and the mean grain size is comparable to or less than the electron MFP, the effect of grain-boundary scattering on the thermal conductivity must be included. By assuming that the grain boundary can be represented by a δ-function potential, Mayadas and Shatzkes studied the grain-boundary effect on the electrical conductivity of polycrystalline metals within the framework of the Boltzmann transport equation. With the electrical–thermal transport analogy, Qiu and Tien obtained the ratio of polycrystalline to single-crystal bulk thermal conductivity as

$$\frac{\lambda_{b,g}}{\lambda_b} = 1 - \frac{3}{2}\alpha + 3\alpha^2 - 3\alpha^3 \ln\left(1 + \frac{1}{\alpha}\right), \tag{12}$$

where $\lambda_{b,g}$ and λ_b are the polycrystalline and single-crystal bulk thermal conductivities respectively and α is a combined parameter which includes the relative magnitude of the mean grain size, i.e. d/l_b, and the reflection coefficient R of the conduction electrons striking the grain boundary, and can be written as $\alpha = l_b R/d(1 - R)$.

By including the background and grain-boundary scattering simultaneously, the effective relaxation time $\tau_{b,g}$ of polycrystalline bulk metals can be obtained from the Matthiessen rule as

$$\frac{1}{\tau_{b,g}} = \frac{1}{\tau_b} + \frac{1}{\tau_g}, \tag{13}$$

where $\tau_{b,g} = l_{b,g}/v_F$, $\tau_g = d/v_F$, τ_g is the relaxation time caused by grain-boundary scattering, and $l_{b,g}$ is the MFP of the polycrystalline bulk metals. The expression for the ratio of polycrystalline to single-crystal thermal conductivities can then be obtained as

$$\frac{\lambda_{b,g}}{\lambda_b} = \frac{l_{b,g}}{l_b} = \frac{1}{1 + l_b/d}. \tag{14}$$

3.3. Combination of surface and grain-boundary effects

For polycrystalline metallic thin films where the film thickness and the mean grain size are both comparable to or less than the MFP, the effects of surface and grain-boundary scatterings on the thermal conductivity should be considered simultaneously. The electron reflection at the surface is usually considered to be completely diffusive, i.e. $p = 0$, in the polycrystalline metallic thin film. The ratio of polycrystalline metallic thin films to single-crystal bulk thermal conductivities, i.e. λ_f/λ_b, can be obtained by the Qiu and Tien model, the KV theory and the relaxation time model as equations (15), (16) and (17) respectively

$$\frac{\lambda_f}{\lambda_b} = \left[1 + \frac{3}{8}\frac{1}{k} + \frac{7}{5}\alpha\right]^{-1}, \qquad k > 0.1, \quad \alpha < 10, \tag{15}$$

$$\frac{\lambda_f}{\lambda_b} = \frac{1}{1 + l_b/d}\left[1 - \frac{3}{8}\frac{1}{k + \delta/d}\right], \qquad k + \delta/d > 1, \tag{16}$$

$$\frac{\lambda_f}{\lambda_b} = \frac{1}{1 + l_b/\delta + l_b/d}. \tag{17}$$

4. Results and discussion

The microstructure of the nanofilms has been studied by x-ray diffraction (XRD) and figure 6 shows the XRD spectra of platinum nanofilms with the thicknesses of 15.0 and 62.0 nm,

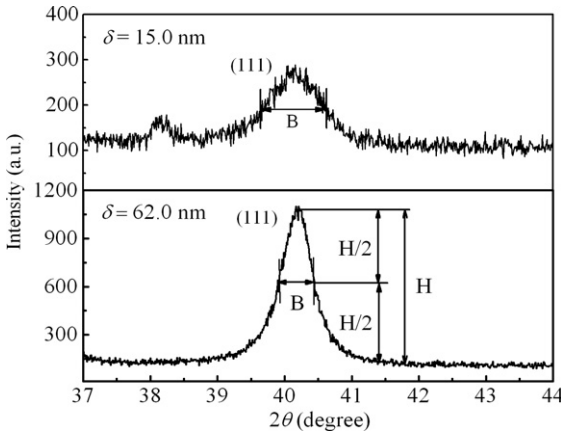

Figure 6. X-ray diffraction spectra of platinum nanofilms with the thickness of (a) 15.0 nm and (b) 62.0 nm.

respectively. It is found that both (111) diffraction peaks are rather broader than the expected sharp peak occurring in the bulk material, indicating that crystallites with finite size exist in the present nanofilms. In the XRD spectrum of 15.0 nm, there is an additional diffraction peak around $2\theta = 38°$, which is found to correspond to Ag(111). In consideration that the platinum specimen is highly pure in the present study (i.e. 99.999%), such a contamination is considered to be introduced in the measurement. Fulmargin is used as an adhesive to join the wires and four nanofilm leads and some must remain on the nanofilms before being studied by XRD. Fortunately, the contamination introduced will not affect the observed mean grain size, as well as the measured thermal conductivity of platinum nanofilms. The average size of the crystallites can be estimated from the full width at half maximum (FWHM) of the peaks using the Scherrer equation as

$$d = \frac{s\lambda_x}{B\cos\theta}, \tag{18}$$

where d is the mean grain size perpendicular to the reflecting plane, B is the FWHM, s is a constant (shape factor) with a value of 0.89, θ is the diffraction angle, and λ_x is the wavelength of the x-ray ($\lambda_x = 0.1541$ nm). With the Scherrer equation, the out-of-plane mean grain sizes of the nanofilms are calculated, and the results are shown in figure 7. It is found that the mean grain sizes are always smaller than the corresponding thicknesses and tend to increase with increasing nanofilm thickness. The unexpected low thermal conductivity of the 62.0–63.0 nm thick nanofilms is considered to be caused by the increased deposition rate from 0.08 to 0.10–0.11 nm s^{-1}. It should be noted that in the latter theoretical calculations the out-of-plane mean grain sizes obtained from XRD studies have been used, while the in-plane mean grain sizes are actually needed. Such a substitution is acceptable in consideration that the in-plane mean grain size is close to the out-of-plane value and an approximately equiaxed microstructure can be observed intuitively from the inserted TEM micrograph as shown in figure 7.

The thermal conductivity of the platinum nanofilms has been measured by the direct electrical heating method, and the temperature changes from 80 to 300 K. The thickness-dependent thermal conductivity at 300 K and the temperature-dependent thermal conductivity for the thickness of 62.0 nm are shown in figures 8 and 9, respectively. It is found from figure 8 that the thermal conductivity has been greatly reduced for all studied nanofilms and tends to increase with increasing nanofilm thickness. The tendency becomes flat when the

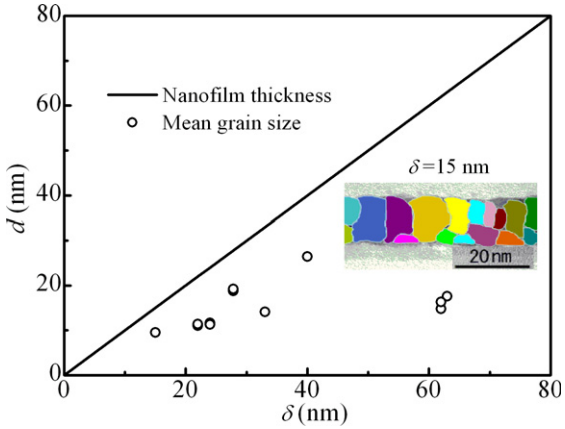

Figure 7. The variation of the mean grain size obtained by XRD studies along the nanofilm thickness. The inset micrograph is obtained from TEM studies, which corresponds to the nanofilm with the thickness of 15.0 nm.

(This figure is in colour only in the electronic version)

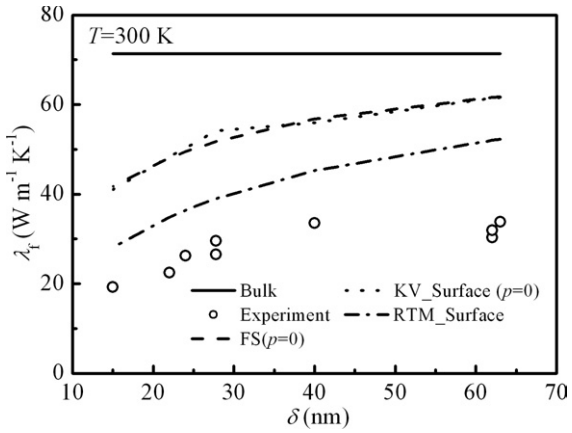

Figure 8. The variations of the thermal conductivity along the nanofilm thickness at 300 K, including the experimental results, the theoretical predictions made by the FS theory, the KV theory and the relaxation time model. The bulk value is also included.

thickness is over about 40.0 nm. The asymptotic thermal conductivity is 33.8 W m^{-1} K^{-1}, which is much less than the bulk value 71.4 W m^{-1} K^{-1}. It is found from figure 9 that the thermal conductivity of the nanofilm increases with increasing temperature, and becomes almost flat around 300 K. Such a tendency in the nanofilm is quite different from that in the bulk material, where the thermal conductivity decreases with increasing temperature. Since the thicknesses and the mean grain sizes of the nanofilms are comparable to the electron MFP of platinum, the deviations of the nanofilm thermal conductivities from the bulk values are attributed to both surface and grain-boundary scatterings. By applying the Qiu and Tien model, the KV theory and the relaxation time model, we studied the surface and grain-boundary effects independently and simultaneously to find out the relative magnitudes of these effects and to examine whether the Matthiessen rule is still valid in predicting the thermal conductivity of the metallic thin films.

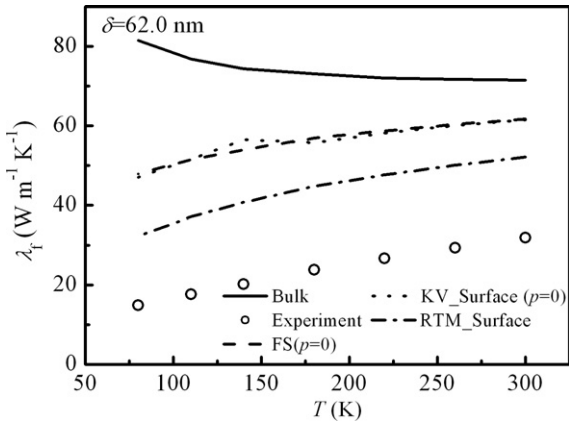

Figure 9. The variations of the thermal conductivity along the temperature for the nanofilm with the thickness of 62.0 nm, including the experimental results, the theoretical predictions made by the FS theory, the KV theory and the relaxation time model. The bulk value is also included.

By considering only the surface effect, the thermal conductivities have been calculated through equations (7), (8) and (10). The obtained variations of the thermal conductivity with the thickness at 300 K and with the temperature for the 62.0 nm thick nanofilm are also shown in figures 8 and 9, respectively. It is found that the thermal conductivities due to the surface effect are reduced from the corresponding bulk values and tend to increase with increasing thickness, as well as increasing the temperature. However, the theoretical predictions obviously overestimate the nanofilm thermal conductivity. In the present calculations the specularly reflected coefficient is taken to be zero, i.e. $p = 0$, which means a completely diffusive surface, and hence the results represent the lowest values that the FS theory and the KV theory can predict. Therefore, other mechanisms leading to the reduction of the thermal conductivity must be considered. It should be noted that the calculated results from the KV theory agree well with those from the FS theory, which coincides with the conclusion drawn from [15]. The results predicted by the relaxation time model, however, are much less than those by the FS theory and the KV theory. It is considered, therefore, that the relaxation time model overestimates the surface effect on the thermal conductivity of the metallic thin films.

With mean grain sizes provided by XRD, the MS theory ($p = 1$) and the relaxation time model, as shown in equations (12) and (14), have been applied to study the grain-boundary effect on the thermal conductivity of polycrystalline bulk metals. The calculated results are shown in figures 10 and 11. It is found that if the reflection coefficient R is taken to be 0.35, the thermal conductivities predicted by the MS theory have been greatly reduced and approximate to the measured values. In the relaxation time model, there are no phenomenology parameters and only size parameters, such as the nanofilm thickness and the mean grain size, are required. The thermal conductivities predicted by the relaxation time model are also greatly decreased from the bulk values and agree with the experimental results with a maximum discrepancy less than 23%. The results indicate that grain-boundary scattering can exert remarkable effects on the thermal conductivity of polycrystalline metals. By including a diffusive surface effect ($p = 0$), the MS theory ($R = 0.35$) and the KV theory, as shown in equations (15) and (16), have been used to study the combined surface and grain-boundary effects on the thermal conductivity of the polycrystalline metallic nanofilms. The calculated thermal conductivities are further diminished as expected compared with those without the surface effect, and coincide with the measured results better. The relative changed values, however, are rather small,

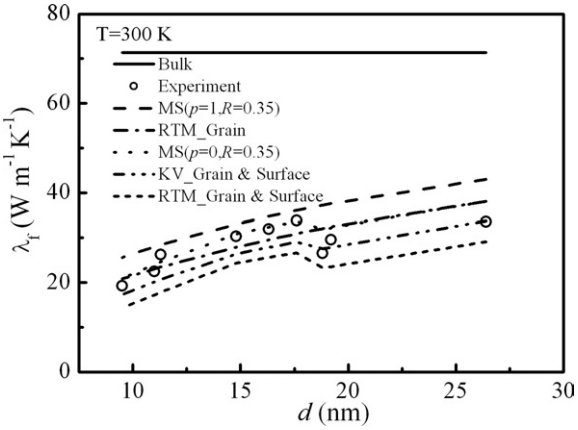

Figure 10. The variations of the thermal conductivity along the mean grain size at 300 K, including the experimental results, the theoretical predictions made by the MS theory with and without the surface effect, the KV theory with the surface effect, and the relaxation time model with and without surface effect. The bulk value is also included.

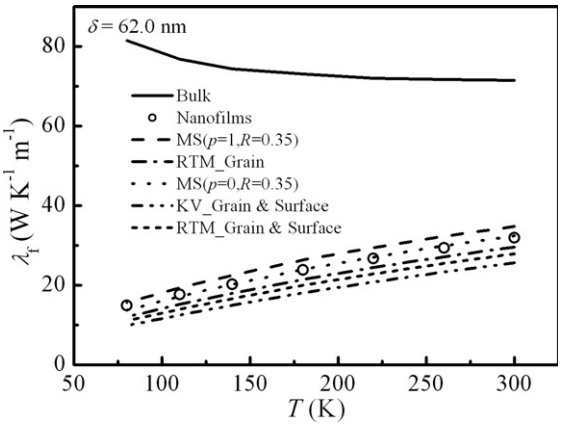

Figure 11. The variations of the thermal conductivity along the temperature for the nanofilm with the thickness of 62.0 nm, including the experimental results, the theoretical predictions made by the MS theory with and without the surface effect, the KV theory with the surface effect, and the relaxation time model with and without surface effect. The bulk value is also included.

with a maximum discrepancy less than 18%. We can conclude from the comparisons that the thermal conductivity is mainly dominated by grain-boundary scattering, and the effect of surface scattering is rather less important. By including the surface scattering mechanism, as well as grain-boundary and background scatterings, the relaxation time model, as shown in equation (17), has also been used to predict the combined size effects on the thermal conductivity. The calculated results are about 10–20% less than those obtained from the KV theory, and also show a deviation from the measured thermal conductivities. The results suggest that the Matthiessen rule will become invalid if surface scattering is included, while it is still satisfied if only grain-boundary and background scatterings are considered. The possible interpretation is given as follows. In the in-plane direction, the effective electron MFP caused

by grain-boundary scattering is determined by the in-plane mean grain size. The corresponding relaxation time can then be expressed by $\tau_g = d/v_F$, as shown in equation (13). For the present nanofilms, the in-plane mean grain size is considered to approximate to the out-of-plane value obtained by the XRD studies. The situation is quite different for surface scattering. The effective mean free path caused only by surface scattering shows great discrepancy in different directions. In the out-of-plane direction the effective mean free path can be regarded as the thickness, while in the in-plane direction it shows a deviation from the thickness and is considered to become larger. Since the in-plane thermal conductivity is concerned in this paper, the relaxation time related to surface scattering cannot be written as $\tau_s = \delta/v_F$, as shown in equation (9). A proper expression is under consideration.

5. Conclusions

The size effects on the in-plane thermal conductivity of the polycrystalline metallic nanofilms have been investigated experimentally and theoretically. The measured results show that the thermal conductivity of the studied nanofilms has been greatly reduced, even down to one-third of the bulk value for the thinnest nanofilms at room temperature and even smaller at lower temperature. By comparing the experimental results with the predictions made by the Qiu and Tien model and the KV theory, we find that the reduction is mainly caused by the grain-boundary scattering, and the contribution of surface scattering is less than 18%. The relaxation time model introduced by the Matthiessen rule has also been used to study the size effects on the in-plane thermal conductivity, which are compared with the predictions made by the Qiu and Tien model and the KV theory, as well as the experimental results. The results indicate that the Matthiessen rule is still valid if only grain-boundary and background scatterings are considered, while it becomes invalid if surface scattering is included. The possible reason is that the effective mean free path caused by grain-boundary scattering can be characterized by the mean grain size, while the effective mean free path induced by surface scattering strongly depends on the direction and cannot be simply characterized by the nanofilm thickness in the direction parallel to the surface.

References

[1] Boiko B T, Pugachev A T and Bratsychin V M 1973 *Thin Solid Films* **17** 157
[2] Nath P and Chopra K L 1973 *Thin Solid Films* **18** 29
[3] Nath P and Chopra K L 1974 *Thin Solid Films* **20** 53
[4] Zhang X, Zhang Q G, Cao B Y, Fujii M, Takahashi K and Ikuta T 2006 *Chin. Phys. Lett.* **23** 936
[5] Kelemen F 1976 *Thin Solid Films* **36** 199
[6] Paddock C A and Eesley G L 1986 *J. Appl. Phys.* **60** 285
[7] Rohde M 1994 *Thin Solid Films* **238** 199
[8] Yamane T, Mori Y, Katayama S and Todoki M 1997 *J. Appl. Phys.* **82** 1153
[9] Tien C L, Armaly B F and Jagannathan P S 1969 *Thermal Conductivity* (New York: Plenum) p 13
[10] Qiu T Q and Tien C L 1993 *J. Heat Transfer* **115** 842
[11] Fuchs K 1938 *Proc. Camb. Phil. Soc.* **34** 100
[12] Sondheimer E H 1952 *Adv. Phys.* **1** 1
[13] Mayadas A F, Shatzkes M and Janak J F 1969 *Appl. Phys. Lett.* **14** 345
[14] Mayadas A F and Shatzkes M 1970 *Phys. Rev.* B **1** 1382
[15] Kumar S and Vradis G C 1994 *J. Heat Transfer* **116** 28
[16] Ziman J M 1960 *Electrons and Phonons, the Theory of Transport Phenomena in Solids* (Oxford: Clarendon) p 260
[17] Tien C L, Majumdar A and Gerner F M 1997 *Microscale Energy Transport* (Washington: Taylor and Francis) p 28

[18] Durkan C and Welland M E 2000 *Phys. Rev.* B **61** 14215
[19] Zhang X, Xie H Q, Fujii M, Ago H, Takahashi K, Ikuta T, Abe H and Shimizu T 2005 *Appl. Phys. Lett.* **86** 171912
[20] Zhang X, Xie H Q, Fujii M, Takahashi K, Ago H, Shimizu T and Abe H 2005 *Japan. J. Thermophys. Prop.* **19** 9
[21] Cahill D G, Katiyar M and Abelson J R 1994 *Phys. Rev.* B **50** 6077
[22] Lee S M and Cahill D G 1997 *J. Appl. Phys.* **81** 2590